

# Effect of Dopants on Arsenic Precipitation in GaAs Deposited at Low Temperatures

V. MAHADEV, M.R. MELLOCH,\* J.M. WOODALL,\* N. OTSUKA,  
and G.L. LIEDL

1289 MSEE Building, School of Materials Engineering, \*School of Electrical Engineering, Purdue University, West Lafayette, IN 47907

High resolution x-ray diffraction using synchrotron radiation was used to characterize GaAs grown by MBE at low temperatures (LT-GaAs). LT-GaAs grown at 225°C is nonstoichiometric and exhibits a 0.15% lattice expansion along the growth direction. Annealing LT-GaAs results in arsenic clusters with a well-defined orientation relationship with the GaAs matrix and a relaxation of the LT-GaAs lattice. The arsenic precipitation corresponds to a classical case of diffusion controlled nucleation and growth followed by coarsening. While the rates of growth and coarsening in the n-doped and the p-doped samples are observed to be identical, the effects of the superlattice seem to accelerate the precipitation kinetics in the p-n superlattice sample. The enhanced coarsening in the p-n superlattice sample is consistent with a previously proposed model involving interaction between charged precipitate and arsenic defects.

**Key words:** Coarsening, dopants, low temperature GaAs, precipitates

## INTRODUCTION

GaAs is normally grown by molecular beam epitaxy (MBE) at substrate temperatures between 580–600°C in order to produce material with a low concentration of deep traps. It is also known that lower growth temperatures (less than 500°C) lead to a very high concentration of deep traps.<sup>1</sup> However, in 1978, Murotani et al.<sup>2</sup> suggested that GaAs grown at low temperatures (LT-GaAs) is semi-insulating even when doped heavily. Subsequently, a paper by Smith et al.<sup>3</sup> in 1988 showed that backgating and light sensitivity could be eliminated by growing a GaAs buffer layer at 200°C and annealing at 600°C. This discovery sparked a lot of interest in LT-GaAs.

GaAs grown by MBE at low substrate temperatures (200–250°C) is in itself not semi-insulating without an anneal at temperatures above 500°C.<sup>4</sup> In fact LT-GaAs with about 1–2% excess arsenic<sup>5</sup> shows changes in several properties on annealing. For ex-

ample, the lattice constant of LT-GaAs, which is about 0.15–0.2% larger than the lattice constant of the substrate, returns to normal on annealing. Also, the arsenic on gallium site ( $As_{Ga}$ ) defect concentration and related quantities are considerably reduced. This reduction in the  $As_{Ga}$  defects is a result of the precipitation of As in annealed LT-GaAs.<sup>6</sup> This interesting observation has fueled an intensive study<sup>7,8</sup> into the properties of these precipitates and their role in the compensation and conductivity of LT-GaAs. In addition to the semi-insulating property, annealed LT-GaAs also has high carrier mobilities and low carrier lifetimes making it a useful material for photoconductive switches.<sup>9</sup>

The effect of doping on the dynamics of arsenic clustering in annealed LT-GaAs was studied by Melloch et al.<sup>10</sup> and Look et al.<sup>11</sup> Melloch et al.<sup>10</sup> observed that the precipitates tend to accumulate in the n-doped regions and deplete from the p-doped regions on annealing, rather than uniformly in the whole region. This was explained as a self-compensation driving mechanism. They suggest that the posi-

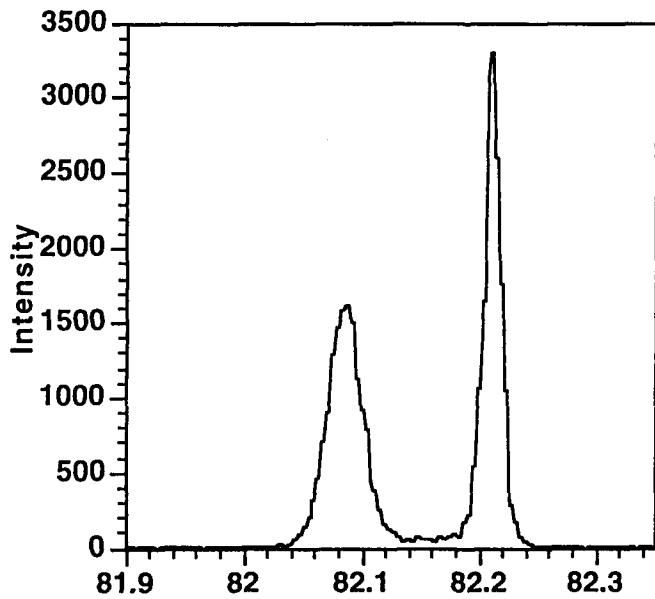


Fig. 1. X-ray  $\theta/2\theta$  scan of the (004) reflections in the as-grown n(p)-doped LT-GaAs sample. Lower angle peak shows broadening from the LT-GaAs film.

**Table I. Lattice Expansion of LT-GaAs Relative to the Substrate as a Function of RTA Temperatures**

Annealing Temp. °C (Time 30 s)	$\Delta a/a$ (%) (n- and p-doped Samples)	$\Delta a/a$ (%) (p-n Superlattice) <u>Expansion Region</u>	
		Lower	Higher
As-Grown	0.151	0.136	0.153
500	0.139	—	—
600	0.093	0.097	0.097
700	0.06	0.0	0.0
800	0.00	0.0	0.0

Note: p-doped and n-doped LT-GaAs have identical lattice expansions.

tively charged As interstitials are attracted to the negatively charged precipitates in the n-doped region and are repelled by the positively charged precipitates in the p-doped regions. However, Look et al.<sup>11</sup> believe that isolated As interstitials do not have donor levels in the upper gap and are not stable, and, therefore, move immediately to precipitates or other sinks. Their conclusion is based on the fact that the As antisites alone are sufficient to account for all the electrically active donors. In fact, at no point in the annealing cycle does donor concentration ( $N_D$ ) increase significantly. However, the interpretation of the data is still open to question since there is very little information available on the effect of annealing at temperatures beyond 700°C. Thus, it is clear that more work needs to be done to understand the effect of dopants on As precipitation in annealed LT-GaAs. If the observation of Melloch et al.<sup>10</sup> that both the charge of the As interstitial and the concentration gradient play a role in the precipitation of arsenic in LT-GaAs, then different growth and coarsening ki-

netics should be observed in the p and n doped samples. The objective of the present study is to probe the effect of dopant type on the kinetics of As precipitation.

## EXPERIMENTAL PROCEDURE

All the samples used in this study were grown in a Varian GEN II MBE system on a  $\langle 001 \rangle$  GaAs substrate. The arsenic flux used was the dimer  $As_2$ , and Si and Be were used as the n-type and p-type dopants, respectively. All layers were grown at the rate of 1  $\mu\text{m}/\text{h}$  with an As to Ga beam-equivalent-pressure ratio of 20. The substrate growth temperature was 225°C. Film thicknesses were about 2  $\mu\text{m}$  for the p-doped ( $2 \times 10^{18}/\text{cm}^3$ ) and n-doped ( $2 \times 10^{18}/\text{cm}^3$ ) samples. A stack of six alternating layers of p-doped and n-doped of 0.2  $\mu\text{m}$  thickness each was used for the p-n sample. Growth and structural details of this sample are explained elsewhere.<sup>10</sup> The samples were then annealed at temperatures ranging between 700 and 1000°C for various lengths of time. The 30 s anneals were conducted in a computer-controlled mini-pulse rapid thermal annealer (RTA). Annealing temperatures and times were chosen to correlate our results with prior transmission electron microscopy (TEM) experiments.<sup>12</sup>

The high resolution x-ray scattering measurements were collected using the X-18A beam line of MATRIX, a midwestern consortium at the National Synchrotron Light Source, Brookhaven National Laboratory. The scattering was measured using a Huber four-circle diffractometer. The focused, monochromatic incoming beam was defined to be  $2 \times 2$  mm on the sample, by a set of incident slits. Scatter slits and receiving slits were set to  $4 \times 4$  mm at 80 and 500 mm from the sample, respectively. A cylindrical mirror focused the beam with energy of the radiation being selected to be 8000 eV using a silicon double crystal monochromator.

## RESULTS

X-ray diffraction data of the as-grown LT-GaAs shows the (004) reflection shifting to a smaller  $2\theta$  angle relative to bulk GaAs, indicating an expansion in the lattice parameter of the n(p)-doped LT-GaAs, due to the excess As incorporation. The LT-GaAs lattice expansion was estimated to be about 0.15%, along [001], the growth direction. The distortion was confirmed to be tetragonal by studying asymmetric reflections of LT-GaAs, such as (224). No distortion was observed in the [H00] and [0K0] directions. Figure 1 illustrates a typical  $\theta/2\theta$  radial scan through the (004) peak of the substrate, for the as-grown n-doped LT-GaAs sample. The broader peak is from the LT-GaAs. Similar results were observed in the p-doped sample. However, in the p-n heterostructure, three peaks were observed in the  $\theta/2\theta$  radial scan through the (004) substrate reflection, indicating two distinct LT-GaAs regions with different lattice parameters.

The LT-GaAs lattice is observed to relax on annealing at temperatures above 500°C, as indicated by

shifting of the LT-GaAs peak toward the bulk GaAs peak location. Annealing at temperatures of 700°C and above, causes the lattice of the LT-GaAs samples to completely relax back to the substrate lattice, as is characterized by a single sharp (004) peak. The measured lattice expansions in the LT-GaAs films for the p-doped, n-doped, and the p-n heterostructure samples are listed in Table I. The measured values of lattice expansions in the p-doped and the n-doped samples were observed to be identical for all annealing conditions. Further, both the as-grown and the annealed samples show distinct interference fringes in the (004) rocking curves, indicating that the films are of excellent structural quality. The structural quality of the LT-GaAs films have been ascertained to be of extremely good quality by double and triple crystal diffraction analyses by Matyi et al.<sup>13</sup> LT-GaAs layer thicknesses were estimated from the angular separation of these interference fringes to be 2 μm for the p-doped and n-doped samples, respectively. This value agrees well with prior TEM measurements on these samples.<sup>12</sup>

The relaxation in the LT-GaAs lattice on annealing is observed to be accompanied by precipitation of the excess As from the matrix. Several reflections from the arsenic precipitate and the matrix were located to determine the orientation relationship between the GaAs matrix and the precipitate. Some of the {01.2}, {01.1}, {01.4}, and the (00.3) reflections of the precipitate and all the {111}, {311}, {220}, {002}, and {004} reflections of the GaAs matrix were located and were the basis for the regression calculation to obtain the orientation matrices of each variant of the precipitate and the matrix, respectively. Analyses of the precipitate phase reflections, corresponds to a hexagonal lattice with the lattice parameters  $a = 3.76\text{Å}$  and  $c = 10.55\text{Å}$ . The orientation relationship between the precipitate and the matrix was determined to be:

$$(0003)_{\text{As}} \parallel (1\bar{1}1)_{\text{GaAs}}, \text{ and } [1\bar{2}10]_{\text{As}} \parallel [110]_{\text{GaAs}} \quad (1)$$

Overall, four orientation variants are possible, consistent with the equivalent {111} planes of the matrix. Our experiments indicate that all four of these variants are present. This observation is in good agreement with the TEM study by Weber et al.<sup>14</sup> Verification of the orientation relationship was obtained by reciprocal lattice radial scans through the maxima of the {111} reflections of the matrix, and through the maxima of the (00.3) reflections of the precipitate, indicating the lack of any misorientation between the (00.3) of the precipitate and the (111) of the matrix. Further, our measurement of the location of the (10.2) of As precipitate indicates that it makes an angle of 11.46° with the other set of {111} planes, consistent with the theoretical calculations. These observations are in contrast with the small misorientation between the (00.3) of the precipitate and the (111) of the matrix reported by Weber et al.<sup>14</sup>

The volume fraction of the As precipitate was determined by comparing the integrated intensities of the

(00.3) reflections of As to the integrated intensities of the GaAs (111) reflections. The ratio of the intensities can be written in terms of the Lorentz-polarization factor (LP) and the structure factor (F) as:

$$\frac{I_{0003}}{I_{111}} = \frac{LP_{0003}}{LP_{111}} \left( \frac{F_{\text{As}}^{0003}}{F_{\text{GaAs}}^{111}} \right)^2 \quad (2)$$

where the square of the structure factor, F, is scaled by the volume fraction,  $V_p$ , of the precipitate as

$$F_{\text{As}}^2 = V_f (F_{\text{As}}^{\text{Tot}})^2 \quad (3a)$$

$$F_{\text{GaAs}}^2 = (1 - V_f) (F_{\text{GaAs}}^{\text{Tot}})^2 \quad (3b)$$

Relative intensities of the variant diffraction peaks indicate that all variants are present in approximately the same amount. The amount of excess arsenic incorporated is estimated to be about 1.50 volume %. The measured precipitate volume fractions are listed as a function of the annealing conditions in Table II. As shown in Table II, the precipitate volume fraction remains a constant after annealing for 30 min at 600°C and for all times at 700°C and higher. These values agree well with that observed in other studies.<sup>12</sup>

The particle size of the arsenic precipitates for the sample aged at 700°C was estimated by measuring the full width at half maximum (FWHM) of the (00.3) reflections of the As phase. The data was corrected for instrumental broadening, which was estimated from the intensity profile of a  $\theta/2\theta$  scan of the bulk GaAs fundamental reflection. The determination of the average particle size from the superlattice reflection is based on the fact that the broadening of the intensity vs  $2\theta$  profile is a function of the particle size of the As precipitates. The full width of the profile corrected for instrumental broadening at half maximum intensity is related to the particle size as:<sup>15</sup>

**Table II. Variation of Particle Size,  $\bar{r}$ , and Volume Fraction,  $V_p$ , of the As Precipitates as of Function of Annealing Conditions**

Anneal Time	600°C		700°C		800°C	
	$V_f(\%)$	$\bar{r}\text{Å}$	$V_f(\%)$	$\bar{r}\text{Å}$	$V_f(\%)$	$\bar{r}\text{Å}$
30 s	1.08	39	1.43	61	1.46	96
5 min	1.21	43	1.42	70	1.43	103
10 min	1.34	49			1.48	111
15 min	1.42	52				
20 min	1.43	57				
30 min			1.46	79		
1 h	1.44	70				
2 h	1.46	78				
3 h	1.44	86	1.45	88		
4 h	1.48	91				
10 h			1.44	103		

Note: The measured values were found to be identical in the p-doped and n-doped samples.

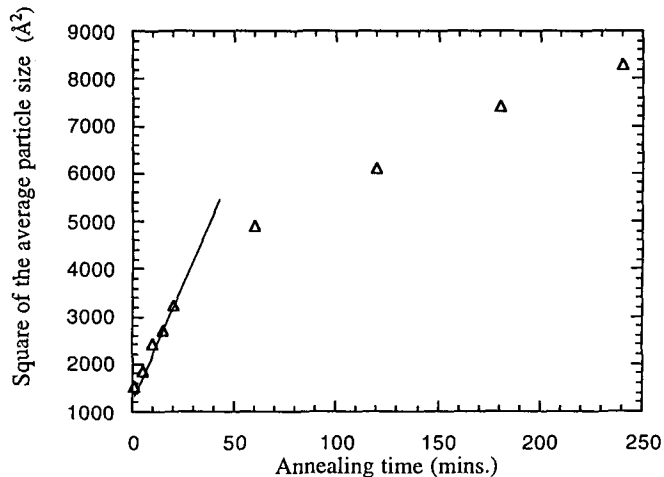


Fig. 2. Variation of the square of the particle size as a function of annealing time at 600°C in p-doped and n-doped samples.

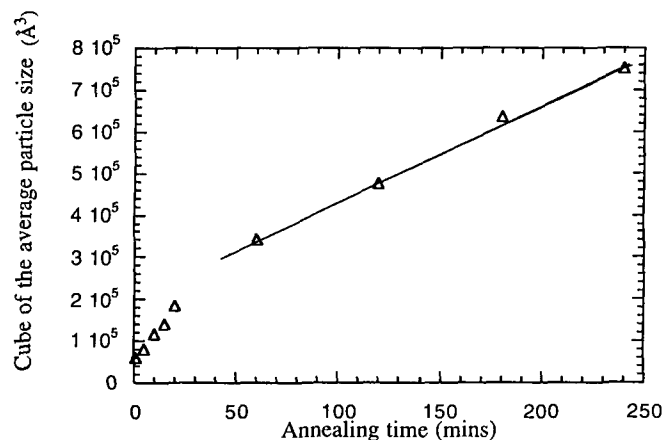


Fig. 3. Variation of the cube of the particle size as a function of annealing time at 600°C in the p-doped and n-doped samples.

$$\bar{r} = \frac{0.46\lambda}{(\text{FWHM}) \cos(\theta_B)} \quad (4)$$

where,  $\lambda$  is the wave length of the incident x-ray beam,  $\theta_B$  is the Bragg angle of the diffraction peak of the As precipitate, and  $\bar{r}$  is the average particle diameter of the As precipitate. This calculation assumes particle size broadening only. Table II lists the calculated values of the average particle size of the As precipitate for various annealing conditions. The volume fraction and the particle size of the precipitate in the n-doped and p-doped samples were identical for all annealing conditions. While the volume fraction of the precipitate was identical in the p-doped and the n-doped samples, the particle size was measured to be higher for similar annealing conditions in the p-n superlattice sample. Average particle diameters of 78, 116, and 168Å were calculated for p-n samples annealed at 700, 800, and 900°C, respectively, for 30 s.

## DISCUSSION

This study has clearly shown that an arsenic phase with a hexagonal structure precipitates upon annealing LT-GaAs and has a definite orientation relation-

ship with the matrix viz.  $(00.3)A_s$  is parallel to the  $(111)$  GaAs. For this orientation relationship, four variants exist and are all observed. The lattice parameters of the As phase were found using high resolution x-ray scattering to be  $a = 3.76\text{\AA}$  and  $c = 10.55\text{\AA}$ . These observations are in agreement with the previous observations made using TEM.<sup>14</sup> However, small volumes of other lower symmetry and amorphous phases observed in other studies were not observed in our experiments.

Also, there seems to be a correlation between the amounts of excess arsenic incorporated in the LT-GaAs lattice and the observed lattice expansion. Tables I and II show the decrease in lattice parameter and increase in the volume fraction of the precipitate with increasing annealing temperature and time. The lack of any detectable lattice expansion on annealing for 15 min at 700°C and for all times above 800°C indicates that all of the excess As has precipitated. This is also confirmed by the fact that the measured volume fraction of the precipitated As remains constant beyond the above-mentioned annealing conditions. Also, the change in the lattice mismatch on annealing at 500°C indicates the onset of precipitation of As phase. However at this stage, the precipitates are too small and their volume fraction too low to be detected.

From the  $\theta/2\theta$  scans of the  $(004)$  reflections of the p-doped, n-doped, and p-n superlattice structures, an attempt is made to understand the effect of doping on the arsenic incorporation and precipitation. The p-doped and the n-doped samples grown using identical growth parameters show the same lattice expansion and excess As incorporation. Samples grown at different substrate mismatches and amounts of excess As incorporation. The p-n sample showed a three-peak  $(004)$  reflection as compared to the two peaks observed in the n(p)-doped samples. The two broadened peaks were associated with the n-doped and the p-doped regions and were at smaller and different  $2\theta$  angles than the substrate peak. The different lattice expansions observed for the p-doped and the n-doped regions indicate that the amounts of excess arsenic incorporated is slightly different in the different regions of the p-n sample.

The semi-insulating property of the LT-GaAs is explained by approximating the precipitates as metallic Schottky barriers that attract and demobilize the electrons in the n-doped material and holes in the p-doped materials. Therefore, to balance the potential difference ( $\Delta V$ ) between the precipitate of radius  $r_o$  and the semiconductor bulk, a negative charge  $Q = 4\pi\epsilon_o\Delta V$  ( $\epsilon =$  dielectric constant) is required. This charge must be formed from donors surrounding the precipitate, leaving a depleted region of radius  $r_s$ . For charge conservation, we require that

$$\frac{4\pi}{3}(r_s^3 - r_o^3)eN_D = Q \quad (5)$$

Thus, there would be a depleted fraction of the sample

volume,  $f = (4\pi/3)r_s^3 N_p$ , where  $N_p$  is the number of precipitate particles per unit volume. For a fully depleted sample  $f \geq 1$ . Using these relations, one can theoretically estimate the required particle size and distribution for a given concentration of the dopants so as to completely deplete the film and make it semi-insulating. Consequently, if the precipitate particle growth and coarsening kinetics are clearly defined, one can then estimate the annealing conditions to just fully deplete the samples. An attempt was, therefore, made to understand and to determine the factors that effect the kinetics of As precipitation.

According to the Lifshitz and Slyozov theory,<sup>16</sup> the kinetic equation for the growth of the precipitates in the pre-coarsening stage is given by

$$\bar{r}^2 = 2\Delta_0 Dt \quad (6)$$

where  $D$  is the intrinsic diffusion coefficient of the solute in the matrix. This linear variation of  $\bar{r}^2$  with aging time for the early stages is shown in Fig. 2. Using this linear fit in the increasing volume fraction region and assuming that the initial supersaturation  $\Delta_0$  can be approximated as the amount of excess arsenic precipitated in the high temperature anneals, reasonable estimates of the diffusion coefficient,  $3.1 \times 10^{-18} \text{ m}^2/\text{s}$  and  $67.2 \times 10^{-18} \text{ m}^2/\text{s}$  for the 600 and 800°C anneals, are obtained. These results agree well with values reported in the literature.<sup>17</sup>

The expression for the time required for the onset of the coarsening process was derived by Kahlweit et al.<sup>18</sup> assuming that the particle density remains constant during the pre-coarsening stage. This assumption was tested by estimating the particle density from the calculated values of the average particle size and the volume fraction. The As particle density,  $N_o$ , was estimated to be about  $7.5 \times 10^{21}/\text{m}^3$  and was observed not to vary significantly with aging. Therefore, using their prediction, the time for onset of coarsening,  $t_c$  can be given as:

$$t_c = \frac{27}{32\pi} \frac{RT}{D\gamma V_m} \frac{\Delta_0}{C_{eq} N_o} \quad (7)$$

With  $\gamma$  as the interfacial energy,  $C_{eq}$  as the concentration of As in the matrix in equilibrium with an As particle of infinite radius,  $D$  as the diffusion coefficient of the solute in the matrix and  $V_m$  as the molar volume of the precipitate. An estimate of  $t_c$  may be made by estimating the intrinsic diffusion coefficient,  $D$ , from the growth stage and using reasonable values for the other parameters,  $\gamma = 0.014 \text{ J/m}^2$ ,  $\Delta_0 = 0.0175$  and  $C_{eq} = 0.50$ . On this basis, the value of  $t_c$  was calculated to be about 26 min at 600°C, which should correspond to the onset of coarsening.

In the latter stages of aging, the Lifshitz-Slyozov-Wagner theory of Ostwald ripening agrees well with the data. According to this theory, the kinetic equation for particle coarsening is given by

$$(\bar{r}^3 - \bar{r}_o^3) = K_c(t - t_o) \quad (8)$$

where  $\bar{r}_o$  is the radius of the precipitate particles at time  $t_o$  at the onset of the coarsening process, and  $K_c$  is the coarsening rate constant given by

$$K_c = \frac{8\gamma V_m C_{eq} D}{9RT} \quad (9)$$

The observed variation of  $\bar{r}^3$  as a function of time is shown in Fig. 3. Comparing Fig. 2 and Fig. 3, the transition from growth to coarsening can be seen as occurring around 30 min, which agrees well with the time for onset of coarsening calculated above using Kahlweit's expression. The rates of growth and coarsening in the p-doped, n-doped, and p-n doped samples are listed in Table III.

This study has clearly shown that the arsenic precipitation corresponds to the classical case of diffusion controlled nucleation and growth followed by coarsening. Melloch et al.<sup>10</sup> suggested that the electrostatic forces between the positively charged As interstitials and the positively charged precipitates in the p-doped regions and the negatively charged As interstitials and the positively charged precipitates in the n-doped are responsible for the observed depletion of the As from the p-doped region as compared to the n-doped region. If the dopant type alone alters the process of the precipitation in the superlattice sample, then the charge effects should tend to reduce the growth and coarsening rates in the p-doped sample and increase them in the n-doped sample. However, our results indicate that the rates of growth and coarsening in the n-doped and p-doped samples are the same. On the surface this appears to contradict what one would expect from the above mentioned theory.

We compare the results from the superlattice sample of Melloch et al.<sup>10</sup> with our results on the p-n sample. The observed rate of coarsening in the p-n sample, which is a composite effect of the rate of coarsening in all the layers, is higher than what is observed in the n-doped and the p-doped samples. Since the supersaturation in the p-n sample is essentially equal to that for our p-doped and n-doped samples, the increased rates are probably due to the interfaces. Boundary effects which include other phenomena, have been observed to provide precipitation-free zones near the boundary such as noted in the coarsening studies of Al-Li alloys.<sup>19</sup> It is, therefore, not surprising

**Table III. Growth and Coarsening Rates Observed in all the Samples for Different Temperatures of Anneal**

Temp. (°C)	p-n-Doped Sample		p-n Superlattice
	Growth $2\Delta_0 D$ ( $\text{m}^2/\text{s} \times 10^{20}$ )	Coarsening $K_c$ ( $\text{m}^3/\text{s} \times 10^{30}$ )	Coarsening $K_c$ ( $\text{m}^3/\text{s} \times 10^{30}$ )
600	2.7	3.8	—
700	—	24	56
800	—	804	1036

to have a junction field effect on the p-n sample. However, for the existing field, the coarsening kinetics should be exactly reversed. This would mean that there exists a stronger driving mechanism for the depletion of the As from the p-doped region and accumulation in the n-doped region. For example, if one assumes a charge induced motion of the As defects as postulated by Melloch et al.<sup>10</sup>, there would be an increase in the rates due to induced diffusion and or supersaturation. Our results would support the general observation of others that there is depletion on the p-doped side and an accumulation on the n-doped side of the superlattice sample. Further, our results would be consistent with the charge model proposed by Melloch et al.<sup>10</sup>

### CONCLUSION

In summary, we have used high resolution x-ray diffraction to understand the effects on excess As incorporation on the lattice of the LT-GaAs epitaxial layer. Annealing of the LT-GaAs leads to the formation of As precipitates and a simultaneous relaxation of the epilayer lattice. The As precipitation corresponds to a classical case of diffusion controlled growth followed by coarsening. The rates of growth and coarsening of the As particles were studied in n-doped, p-doped, and p-n doped samples for several annealing conditions. While the n-doped and the p-doped samples show similar growth and coarsening kinetics, the p-n sample shows faster kinetics. These observations of the p-n superlattice effect agree well with the model postulated by Melloch et al.<sup>10</sup>

### ACKNOWLEDGMENTS

This research was sponsored by U.S. Department of Energy (contract No. DE-FG02-85ER 45813) and utilized the MATRIX beam line X-18A, at NSLS. This work was also supported by the U.S. Air Force Office of Scientific Research (Grants No. F49620-93-1-0031 and F49620-93-1-0388).

### REFERENCES

1. R.A. Stall, C.E.C. Wood, P.D. Kirchner and L.F. Eastman, *Electron. Lett.* 16, 171 (1980).
2. T. Murotani, T. Shimanoe and S. Mitsui, *J. Cryst. Growth* 45, 302 (1978).
3. F.W. Smith, A.R. Calawa, C.L. Chen, M.J. Manfra and L.J. Mahoney, *IEEE Electron. Device Lett.* 9, 77 (1988).
4. D.C. Look, D.C. Walters, M.O. Manasreh, J.R. Sizelove, C.E. Stutz and K.R. Evans, *Phys. Rev. B* 42, 3578 (1990).
5. M. Kaminska, Z. Liliental-Weber, E.R. Weber, T. George, J.B. Kortright, F.W. Smith, B.Y. Tsaur and A.R. Calawa, *Appl. Phys. Lett.* 54, 1881 (1989).
6. M.R. Melloch, N. Otsuka, J.M. Woodall, A.C. Warren and J.L. Freeouf, *Appl. Phys. Lett.* 57, 1531 (1990).
7. A.C. Warren, J.M. Woodall, J.L. Freeouf, D. Grischkowsky, D.T. McInturff, M.R. Melloch and N. Otsuka, *Appl. Phys. Lett.* 57, 1331 (1990).
8. D.C. Look, *J. Appl. Phys.* 70, 141 (1991).
9. A.C. Warren, N. Katzenellenbogen, D. Grischkowsky, J.M. Woodall, M.R. Melloch and N. Otsuka, *Appl. Phys. Lett.* 58, 1512 (1991).
10. M.R. Melloch, N. Otsuka, K. Mahalingam, C.L. Chang, J.M. Woodall, G.D. Pettit, P.D. Kirchner, F. Cardone, A.C. Warren and N.D. Nolte, *J. Appl. Phys.* 72, 3509 (1992).
11. D.C. Look, D.C. Walters, G.D. Robinson, J.R. Sizelove, M.G. Mier and C.E. Stutz, *J. Appl. Phys.* 74, 306 (1993).
12. C.L. Chang, M.S. Thesis, School of Materials Engineering, Purdue University.
13. R.J. Matyi, M.R. Melloch and J.M. Woodall, *J. Cryst. Growth* 129, 719 (1993).
14. Z. Liliental-Weber, A. Claverie, J. Washburn, F. Smith and R. Calawa, *Appl. Phys. A* 53, 141 (1991).
15. B.E. Warren, ed. *X-Ray Diffraction* (Addison-Wesley Publishing Company), p. 251.
16. I.M. Lifshitz and V.V. Slyozov, *J. Phys. Chem. Sol.* 19, 35 (1961).
17. H.D. Palfrey, M. Brown and A.F.W. Willoughby, *J. Electron. Mater.* 12 (5), 863 (1983).
18. M. Kahlweit, F. Lichtenfeld, R. Strey and J. Jen, *Decomposition of Alloys: The Early Stages*, eds. P. Hansen, V. Gerold, R. Wagner and M.F. Ashby, (Pergamon Press, 1983), p. 61.
19. D.B. Williams, *Proc. Fifth Intl. Conf. on Aluminum-Lithium Alloys*, ed. E. A. Starke and T. H. Sanders, Williamsburg, VA, (1989), p. 551.